Phase Structures, Transition Behaviors, and Surface Alignment in Polymers Containing a Rigid Rodlike Backbone with Flexible Side Chains. 2. Phase Transition Kinetics in a Main-Chain/Side-Chain Liquid Crystalline Polyester

Jason J. Ge, Anqiu Zhang, Kevin W. McCreight, Shy-Yeu Wang, Frank W. Harris, and Stephen Z. D. Cheng*

Maurice Morton Institute and Department of Polymer Science, The University of Akron, Akron, Ohio 44325-3909

Received February 24, 1998; Revised Manuscript Received April 17, 1998

ABSTRACT: A series of polyesters consisting of aromatic main-chain backbones and flexible aliphatic side chains with 4-cyanobiphenyl end groups has been synthesized on the basis of the polycondensation of 2,2′-bis(trifluoromethyl)-4,4′-biphenyldicarbonyl chloride with 2,2′-bis{*ω*-[4-(4-cyanophenyl)phenyoxy]-*n*-alkoxycarbonyl]}-4,4′-biphenyldiol (PEFBP). As recently reported, for a PEFBP polyester containing eleven methylene units in the side chains, PEFBP(*n*=11), four different structures have been identified in addition to the isotropic melt. They are as follows: an orthorhombic crystalline phase (K_O), two triclinic crystalline phases (K_{T1} and K_{T2}) in the high-temperature region, and a nematic phase (N). To further understand the phase transformation mechanisms involved, in this publication, overall phase transformation kinetics have been carried out using isothermal differential scanning calorimety (DSC) experiments. Special attention has been given to the temperature regions where three phases (K_O, K_{T1}, and K_{T2}) exist. It is found that each phase possesses its own transformation rates. Three overall transformation rate regions are observed that are separated at temperatures of 95 and 113 °C, which serve as rate boundaries between these different phases. For the linear growth rates measured by polarized light microscopy (PLM), the growth rate of the K_O phase is difficult to be detected due to its fast transformation rates. The linear growth rates of the K_{T1} and K_{T2} phases can, however, be measured. Although these rate regions generally correspond to the overall transformation rates obtained from DSC, a rate minimum can be observed at 130 °C in the linear growth rate data of the K_{T2} phase above 113 °C. This minimum is formed due to the introduction of a new linear growth rate branch above 130 °C. The morphological studies under PLM, transmission electron microscopy, and the melting temperature changes using DSC indicate that these two growth rate branches in the K_{T2} phase correspond to two kinds of morphological developments: folded chain spherulites and extended chain single crystals. Furthermore, the linear growth rates are affected more by this morphological change compared to the overall transformation rates.

Introduction

Recently, special interest in liquid crystalline polymers (LCPs) has been concentrated on the design of molecular architecture to achieve specific macroscopic properties. To meet particular requirements in liquid crystal display industries and other applications, a new class of main-chain LCPs with flexible side chains has been synthesized.[1−5] Moreover, "combined" main-chain and side-chain LCPs have also been reported.[6−10] The presence of mesogenic units in both the backbone and side chains may lead to intriguing structural organization in the bulk as well as on thin film surfaces.

In the first report of this series of specifically designed polyesters synthesized on the basis of a polycondensation of 2,2′-bis(trifluoromethyl)-4,4′-biphenyldicarbonyl chloride with 2,2′-bis{*ω*-[4-(4-cyanophenyl)phenyoxy]-*n*-alkoxycarbonyl}-4,4′-biphenyldiol (PEFBP), the phase structures and phase transitions of a PEFBP polyester containing eleven methylene units in the side chains, PEFBP(*n*=11), were investigated.[11] The chemical structure of this polymer is

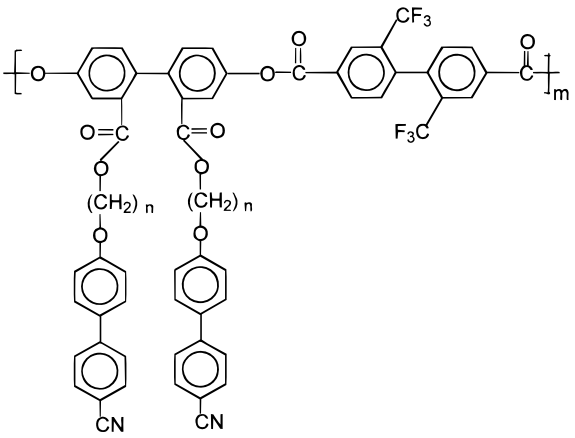

It is found that this "combined" main-chain and side-chain liquid crystal polyester exhibits complicated phase structures.[11] On the basis of our structural analysis, four phases with different ordered structures are involved in this polymer: a two-chain orthorhombic packing (K_O), two four-chain triclinic crystals (K_{T1} and K_{T2}), and a nematic (N) phase, in addition to its isotropic melt. The glass transition temperature of this "com-

* To whom correspondence should be addressed.

S0024-9297(98)00285-X CCC: $15.00
Published on Web 05/23/1998

bined" liquid crystal polyester is 50 °C. When the polymer is slowly cooled to room temperature (such as at 1 °C/min) and reheated to the isotropic melt, the phase transformation sequence is[11]

$$T_g \rightarrow K_O \rightarrow N \rightarrow K_{T1} \rightarrow (N?) \rightarrow K_{T2} \rightarrow N \rightarrow I$$

It is evident that the N phase not only is observed in the high-temperature region but also appears after the melting of the K_O phase and before the formation of the K_{T1} phase. However, we are not yet certain whether this N phase returns after the melting of K_{T1} phase and before the formation of the K_{T2} phase. If this happens, the transformation of the $N \rightarrow K_{T2}$ phases must be very fast and is below the time scale of experimental observations [about 1 min in wide-angle X-ray diffraction (WAXD) experiments]. This phenomenon is an apparent "reentrant" behavior, but it should be noted that this is kinetically controlled due to the monotropic phase behavior of both metastable K_O and K_{T1} phases with respect to the stable K_{T2} phase.[11]

Experimental Section

Materials and Samples. The synthesis of this "combined" liquid crystal polyester was reported in previous publications.[11,12] For a polyester containing eleven methylene units in the side chains as a spacer, its abbreviation is PEFBP-(n=11). The intrinsic viscosity of this polymer is 0.5 dL/g in chloroform at 30 °C. The sample was fractionated using chloroform/methanol solvents. The relative molecular weight of the polymer was determined by gel permeation chromatography based on the polystyrene standard. The number average molecular weight was 15 600, and the polydispersity was 1.1.

Polyester powder samples were used in differential scanning calorimetry (DSC) studies. Films having a typical thickness of a few micrometers were prepared by a solution-casting method from a 1% (w/w) solution in chloroform for polarized light microscopy (PLM) experiments. In particular, monodomains in the film samples were created using mechanical shearing since linear growth rates were measured through crystals grown from the monodomains of the N phase. For transmission electron microscopy (TEM) experiments, thin films (less than 0.3 μm) were prepared using solution-casting of a 0.1% (w/w) solution in chloroform. All of the film samples were dried at room temperature overnight in a vacuum oven before sample thermal treatments.

Equipment and Experiments. DSC was performed on a Mettler DSC-820 with a liquid nitrogen cooling apparatus. The temperature and heat flow were calibrated using standard materials. Isothermal experiments were carried out to study overall phase transformation kinetics. The samples were first heated to 210 °C and kept in the isotropic melt for 2 min. Samples were then quenched to preset isothermal temperatures and held there for different periods of time. Afterward, the samples were heated to the isotropic melt at a rate of 10 °C/min to obtain the heats of transition as a function of time.

To determine the types of ordered structures formed at different isothermal temperatures, WAXD fiber experiments were conducted on a Rigaku 18 kW rotating-anode generator (Cu Kα) coupled with an image plate, and WAXD powder patterns were obtained from a diffractometer on a Rigaku 12 kW rotating-anode generator (Cu Kα). The X-ray beams were monochromatized using well-defined graphite crystals. Hot stages attached to the powder and fiber sample holders allow observations of the change of phase structures with temperature. To improve resolution, the WAXD powder patterns were recorded at a scanning rate of 0.2°/min, and the fiber patterns were taken for a period of 1 h at each temperature. Correlation lengths were calculated on the WAXD powder patterns on the basis of the Scherrer equation as a first approximation with consideration of broadening effects from the instrument. The reflection peak positions and widths observed were calibrated with silicon crystals of known crystal sizes in the high-angle region (2θ > 15°) and silver behenate in the low-angle region (2θ < 15°). The angular deviation measured in WAXD was ±0.05° with an instrumentation function of 0.03°.

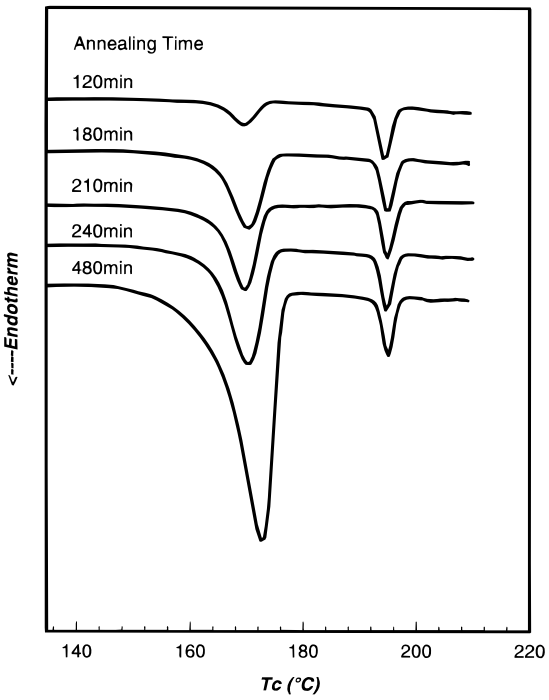

Figure 1. Set of PEBFP(n=11) DSC heating curves after isothermal experiments at 135 °C for different periods of time.

Isothermal experiments were also conducted on a polarized light microscope [Olympus (HB-2)] coupled with a Mettler hot stage FP-90. The thermal histories were the same as those in the DSC experiments. Linear crystal growth rates were measured under PLM by recording the linear dimensional change with respect to time. If two different types of morphologies were observed at one temperature, growth rates for both types of morphologies were measured separately. Note that the growth rates were measured in large liquid crystalline monodomains, since the N phase cannot be bypassed during the quenching process.

A JEOL (1200 EX II) transmission electron microscope was utilized to study the detailed morphological changes in this polyester at different temperatures. The samples were tested under the same thermal conditions as those in DSC and PLM experiments. The samples were quenched in liquid nitrogen, and TEM experiments were carried out at room temperature. The thin films were shadowed by Pt and coated with carbon for TEM observations. An accelerating voltage of 120 kV was used.

Results and Discussion

Overall Phase Transformation Kinetics. Figure 1 shows a set of DSC heating diagrams for PEFBP-(n=11) isothermally held at 135 °C for different periods of time after being quenched from the isotropic melt (again, during quenching, the N phase cannot be bypassed). There are two endotherms in the DSC heating curves. The higher temperature endotherm represents the $N \rightarrow I$ transition while the lower temperature endotherm is attributed to the melting of the K_{T2} crystal structure (see below). It is clear that the heat of transition under the lower temperature endotherm gradually increases, indicating an evolution of this ordered structure during the isothermal experiments. The endothermic temperature increases slightly

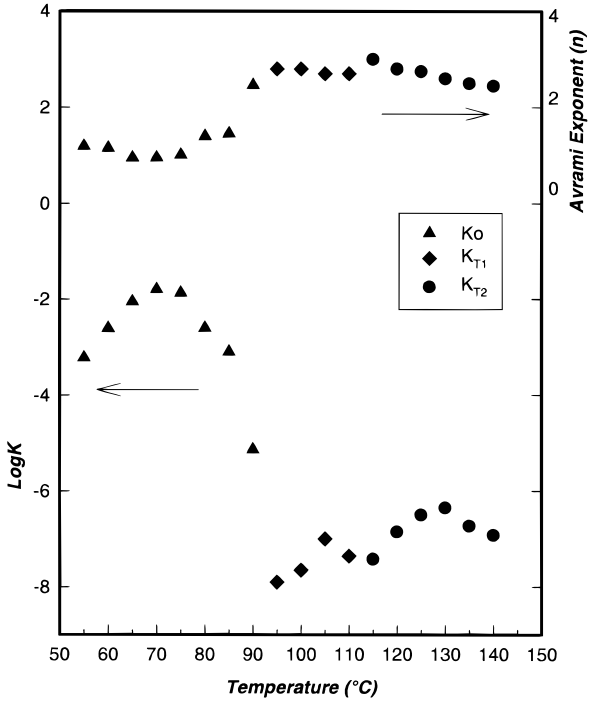

Figure 2. Plot of log K and n with respect to isothermal temperatures in PEBFP(n=11).

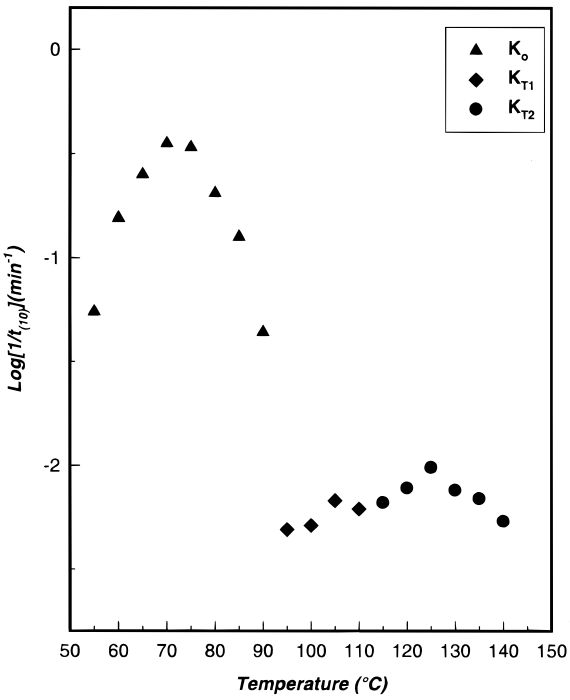

Figure 3. Plot of logarithmic reciprocal time of reaching 10% of the overall heats of transition with respect to isothermal temperature in PEBFP(n=11).

with time due to a crystal perfection process. On the other hand, the heat of transition and the transition temperature of the higher endotherm (the N → I) remain constant and are independent of time, revealing that this transition is close-to-equilibrium in nature.

This kind of experiment was carried out in the temperature region from 55 to 140 °C, where three crystalline phases are included: the K_O, K_{T1} and K_{T2} structures based on the WAXD and electron diffraction analyses.[11] The experimental data can be treated using the Avrami equation ($\log[-(1 - v^c)] = \log K + n \log(t)$, where v^c is a volume crystallinity; for a relative comparison purpose, as in this case, v^c can be replaced by using a weight crystallinity obtained from the DSC results). Two Avrami parameters, the Avrami exponent (n) and prefactor (K), can be deduced. Under the condition that the phase structures, primary nucleation type, and morphology are known (see below), the Avrami exponent n represents the dimension of growth in the ordered structure, while the prefactor K is associated with the geometry of the growth, the number of nuclei, and the n (athermal) or (n + 1) (thermal) power of the linear growth rate. Figure 2 shows log K and n at different temperatures for PEFBP(n=11) over the entire temperature region of the K_O, K_{T1}, and K_{T2} phases under examination, and log K values may represent overall transformation rates.

When we consider the time which is necessary to develop 10% of the ordered structure ($t_{10\%}$), the reciprocals of this time may represent the primary nucleation rate at different temperatures, as shown in Figure 3. From Figures 2 and 3, three apparently independent regions of the overall phase transformation and primary nucleation rates can be found. Two boundaries at 95 and 113 °C are observed among these three regions. These two boundary temperatures correspond well to the transition temperatures between the K_O ↔ K_{T1} phases and the K_{T1} ↔ K_{T2} phases. The low-temperature region in Figures 2 and 3 is associated with the K_O phase formation in the temperature region 55−95 °C, while the high-temperature region is attributed to the crystal phase K_{T2} formation in the temperature region above 113 °C. Between the K_O and K_{T2} phases, the K_{T1} phase forms within a narrow temperature region between 95 and 113 °C.

From Figure 2, an Avrami exponent (n) around 1 is obtained in the low temperature region up to 75 °C. This value then generally increases to 2.8 at 90 °C. It is speculated that, in the K_O phase formation, a morphological change from one-dimensional to three-dimensional growth may take place. It can be confirmed that at 70 °C the ordered structure exhibits a needle-like shape while spherulitic aggregates can be observed above 90 °C (see below). In the K_{T1} phases, the corresponding Avrami exponent (n) is approximately 2.8 and remains constant in the temperature region 95−113 °C. This indicates that the K_{T1} crystallization process is an athermal nucleation-controlled process with approximately three-dimensional growth which can be revealed by PLM results (see below). On the other hand, as the isothermal temperature is further increased to enter the K_{T2} phase, the Avrami exponent (n) decreases from 2.9 at 115 °C to 2.4 at 140 °C. This phenomenon may also be related to a change from three- to two-dimensional crystal growth. In the corresponding PLM observations, a general morphological change has been found from spherulites at 115 °C to close-to-rectangular-shaped single crystals at 140 °C (see below).

As shown in Figure 3, which is a plot of the logarithmic reciprocal times of the 10% development of the heat of the transition in the ordered structures (the primary nucleation rates) versus temperature, it is obvious that each phase has its own structural formation kinetics in different temperature regions. For instance, the K_O phase possesses a much faster rate maximum at around 70 °C (several orders of magnitude) compared to those of the other two phases. The K_{T1} phase exhibits the slowest rate maximum at 105 °C in the narrow tem-

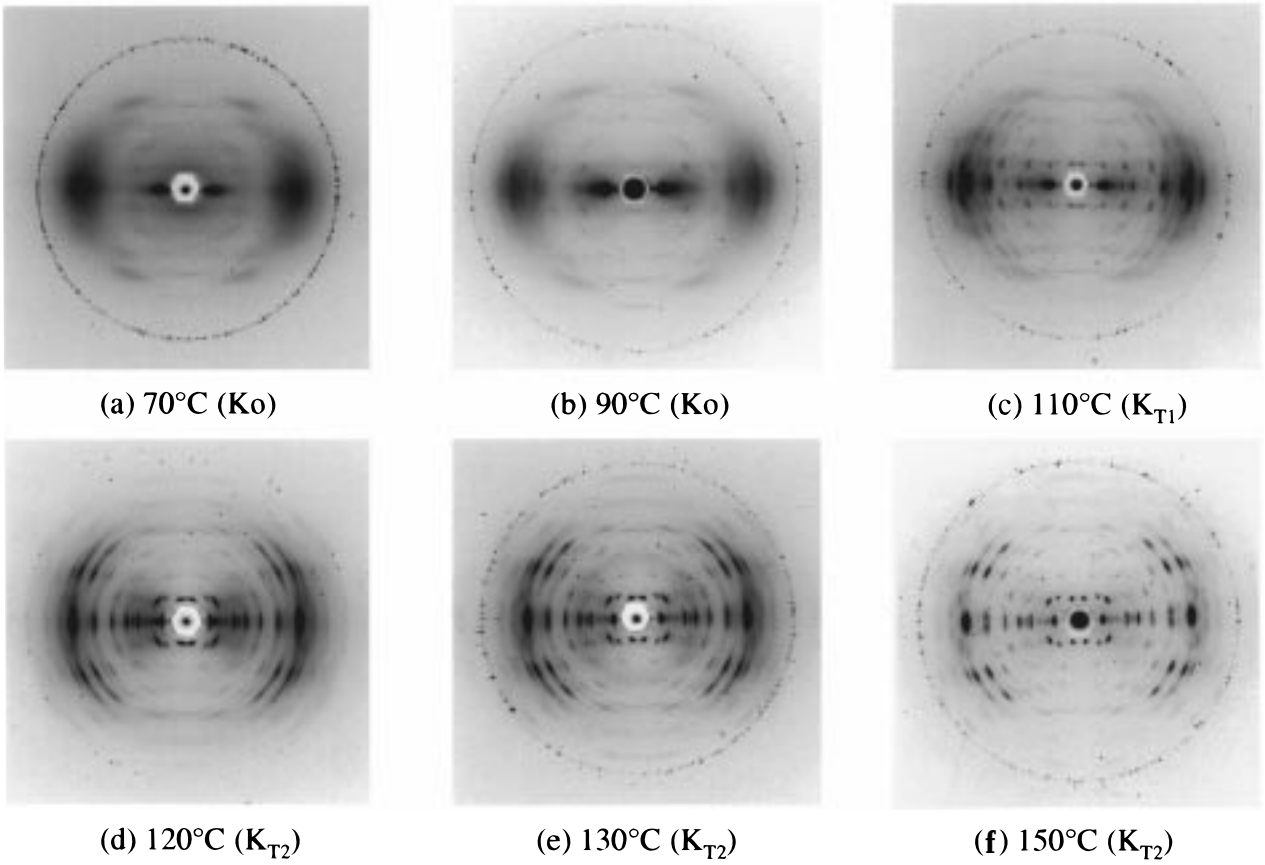

Figure 4. Set of PEBFP(n=11) WAXD fiber patterns of the K_O, K_{T1}, and K_{T2} phases at the isothermal temperatures (a) 70, (b) 90, (c) 110, (d) 120, (e) 130, and (f) 150 °C.

perature region (18 °C) among these three rate regions. This is probably attributed to different phase structures which possess significantly different free energy barrier heights in the phase formation (see below for discussion). The high-temperature region is related to the kinetics of the K_{T2} phase. The rate maximum at 125 °C is faster than that in the K_{T1} phase. However, if one examines the overall transformation rates (log K values) in Figure 2, the high-temperature rate maximum occurs at 130 °C (5 °C shift of the rate-maximum compared with that in Figure 3), and at 140 °C there is a clear but minor upturn of the log K. These apparent differences may be explained after the study of linear growth rates (see below).

Changes of the Phase Structures. To confirm the structure formation in these different phases, isothermal WAXD fiber patterns taken at 70, 90, 110, 120, 130, and 150 °C are shown in Figure 4. At each temperature step, the samples were annealed for an extended period of time (a few days) in order to obtain distinct diffraction patterns with maximum crystallinities in these phases. Their corresponding WAXD powder patterns are shown in Figure 5. On the basis of the previous structural analyses,[11] it is evident that these three regions of the overall transformation and primary nucleation rates in DSC experiments belong to three different phase structures. From Figures 4 and 5, the orthorhombic K_O phase occurs at 70 and 90 °C (Figures 4a and b and 5a and b), the triclinic K_{T1} phase occurs at 110 °C (Figures 4c and 5c), and the triclinic K_{T2} phase occurs from 120 to 150 °C (Figures 4d−f and 5d−f). These WAXD fiber patterns confirm the ordered structures determined in our previous work.[11] Although the unit cell dimensions of the K_{T1} and K_{T2} phases are close to each other and it

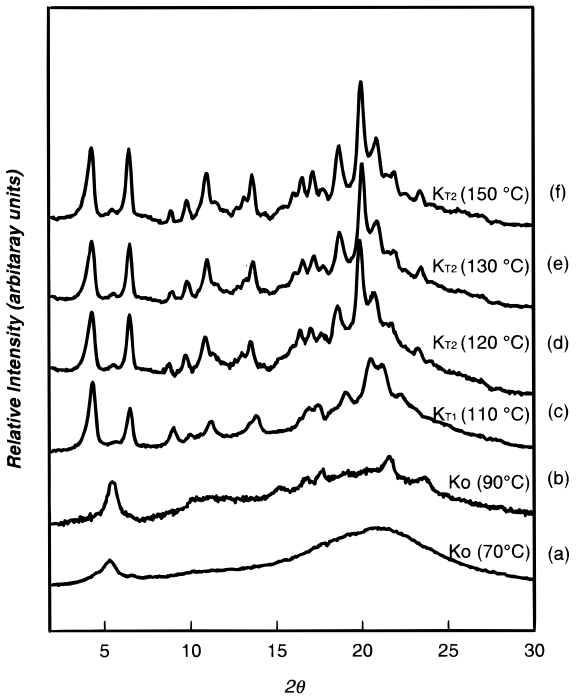

Figure 5. Set of PEBFP(n=11) WAXD powder patterns of the K_O, K_{T1}, and K_{T2} phases at the isothermal temperatures (a) 70, (b) 90, (c) 110, (d) 120, (e) 130, and (f) 150 °C.

was speculated that these two phases may belong to a single phase with slight modification due to the annealing effect,[11] the overall transformation and primary nucleation rates shown in Figures 2 and 3 clearly indicate that these phases possess their own formation

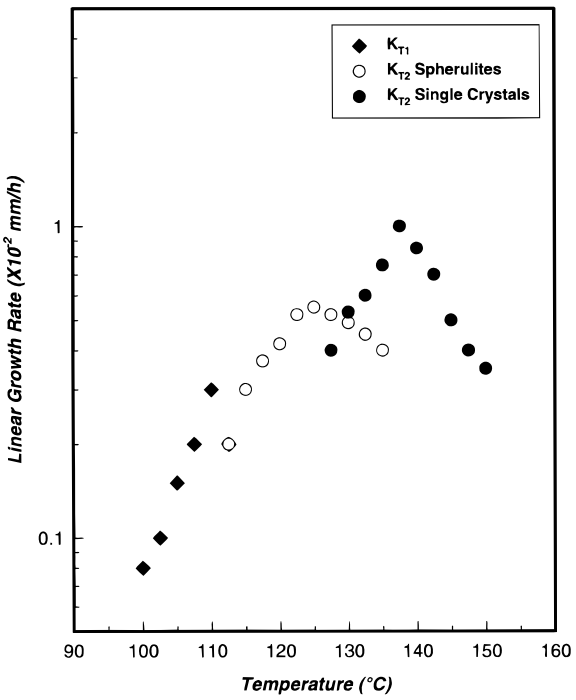

Figure 6. Plot of linear growth rates with respect to isothermal crystallization temperatures in PEBFP(n=11).

kinetics and that they should therefore be independent crystal structures.

Using the Scherrer equation, correlation lengths of the (001) plane can be calculated on the basis of the WAXD powder patterns (Figure 5). Below the isothermal temperature of 130 °C, the correlation lengths are in the range between 12 and 18 nm, depending upon the isothermal temperatures. However, at 150 °C in the K_{T2} phase, the correlation length suddenly increases to approximately 26 nm.

Linear Growth Rates of the Phase Transformations. Figure 6 shows a plot of linear growth rates of PEFBP(n=11) measured under PLM versus isothermal crystallization temperature. Below 95 °C, the linear growth rates of the K_O phase cannot be measured, since only an increase in the birefringence of the liquid crystal-like texture is observed, which may indicate that this phase should be associated with a highly ordered smectic crystal. Therefore, in the linear growth rate measurements, the lowest growth rate region which can be determined is between 95 and 113 °C and is attributed to the K_{T1} phase. Note that this region corresponds to the middle region of the overall transformation and primary nucleation rates in Figures 2 and 3. The maximum linear growth rate branch of the K_{T1} phase is again slower compared to that of the K_{T2} phase. It is surprising that two linear growth rate branches are found in the K_{T2} phase above 113 °C and that a rate minimum at 130 °C is identified. Two rate maxima are observed at 125 and 137.5 °C.

In Figures 2 and 3, however, both the overall transformation and primary nucleation rates of the K_{T2} phase above 113 °C only exhibit a single rate curve. The difference between these two rate regions in both figures is that the maximum rate temperatures show a shift of 5 °C and the upturn of the rate at 140 °C in the overall transformation rate in Figure 2. Furthermore, this upturn overall transformation rate curve occurs when the rate is decreasing. In the linear growth rates shown in Figure 6, the rate maximum at 137.5 °C is about two times faster than that at 125 °C (in an increasing trend). The explanation of these inconsistencies may lie in the experimental observations that, at 140 °C, the primary nucleation barrier of the single lamellar crystals is high (Figure 3) and, therefore, the induction time of the phase formation is long. Since the overall transformation rates in Figure 2 are attributed to both primary nucleation and linear growth steps, the faster linear growth rates are offset by the slower nucleation rates. Threfore, only one rate curve in the overall kinetics data and a minor upturn of the log K can be found.

These dramatic differences indicate that it is possible to miss a significant change in linear crystal growth behavior when one only investigates the overall transformation and /or primary nucleation rates. It should be reiterated that, in this temperature region, WAXD results only show one crystal structure, which is the K_{T2} phase. This difference must be caused not by varying crystal structures but by a morphological change.

Crystal Morphological Changes Between K_O and K_{T1} Phases and Within the K_{T2} Phase. To verify morphological changes in different phases as well as the speculation that the morphological change is the result of these two linear growth rate branches observed in the K_{T2} phase, Figure 7 shows a series of morphological observations under PLM at different temperatures. In Figure 7a, the morphology observed at 90 °C is similar to those found in highly ordered smectic liquid crystalline textures.[13] No spherulitic crystal morphology can be seen. In Figure 7b, there are a number of small spherulitic crystals of the K_{T1} phase grown from the N phase at 100 °C. Some of the spherulites exhibit a unique blue or yellow birefringence after a $^1/_4$ λ compensator is used instead of the normal Maltese crosses. This may indicate that these crystals in the K_{T1} phase possess molecular orientations with either uniform positive or negative birefringence. The formation mechanism by which these molecules align is not yet clear but must be associated with the parent N phase. In Figure 7c, both spherulites and close-to-rectangular single crystals of the K_{T2} phase develop independently at 130 °C from the N phase. This temperature is at the linear growth rate minimum of the two branches within the K_{T2} phase. Both crystals have different morphologies and possess independent linear growth rates. This dual-morphological phenomenon exists in the temperature region between 128 and 135 °C. In the temperature region between 115 and 125 °C, only spherulites of the K_{T2} phase grown from the N phase can be found, and they show somewhat irregular Maltese crosses. In Figure 7d, only close-to-rectangular single crystals of the K_{T2} phase, which have one angle which is close to 80° and a supplementary angle of around 100°, develop above 135 °C.

These corresponding morphological changes in the K_O, K_{T1}, and K_{T2} phases are further confirmed using TEM observations, as shown in Figure 8. In Figure 8a, needle-like aggregates can be found at 80 °C. In Figure 8b, spherulites are seen at 100 °C in the K_{T1} phase, which appear to have cracks perpendicular to the radial direction. This may be caused by anisotropic coefficients of thermal expansion along two different directions in the crystals, as shown in the case of syndiotactic polypropylene.[14,15] At 130 °C, dual-morphologies (spherulitic crystals and single lamellar crystals) can be found

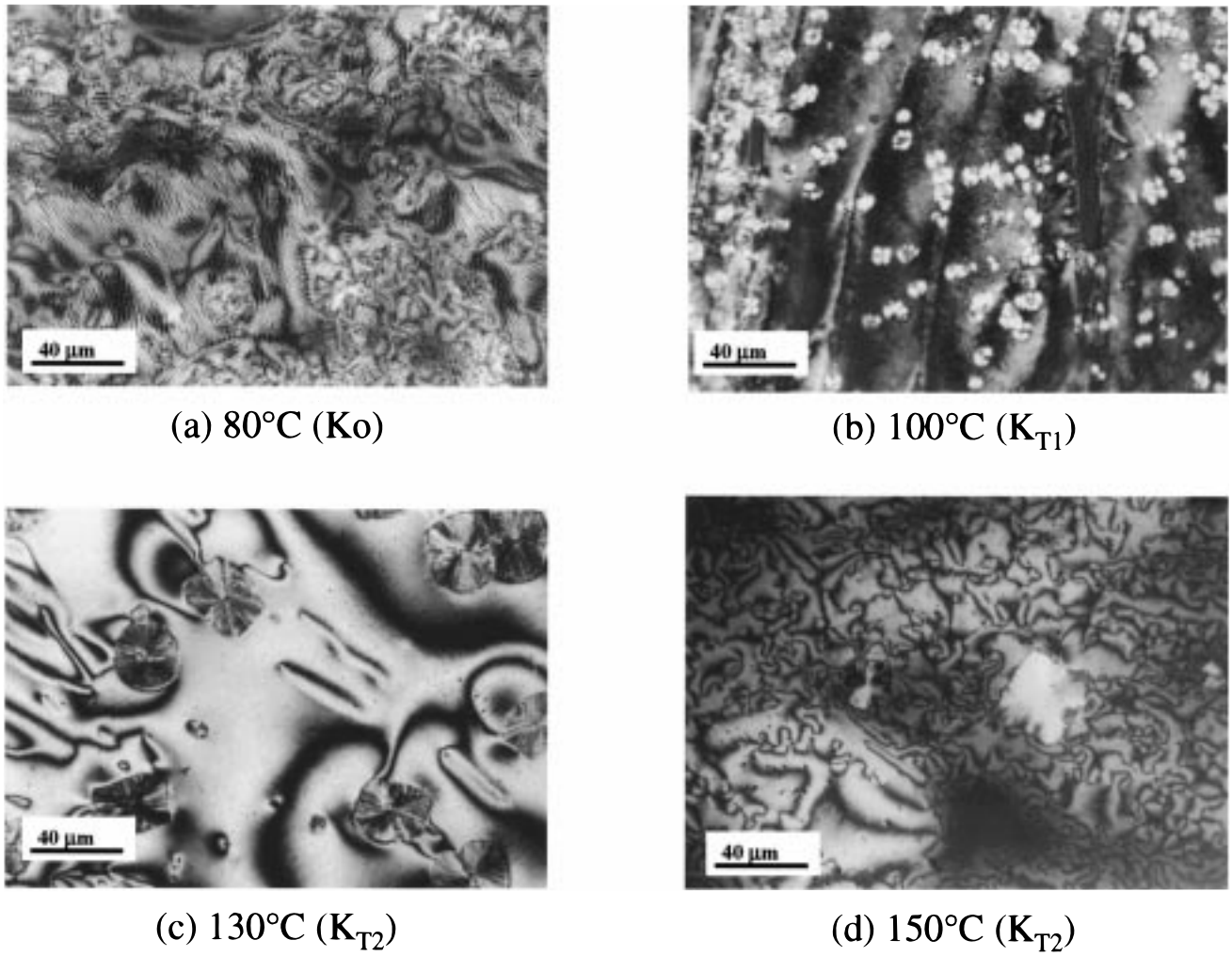

Figure 7. Morphological observations under PLM at different temperatures: (a) the K_O phase at 70 °C; (b) the K_{T1} phase at 100 °C; (c) the K_{T2} phase at 130 °C; (d) single crystals of the K_{T1} phase at 140 °C.

in the K_{T2} phase. In Figure 8c, the top left corner shows part of a spherulite, while the rest of the areas are single lamellar crystals. At 145 °C in the K_{T2} phase, only single lamellar single crystals develop with the close-to-rectangular facets (Figure 8d).

From TEM experiments, the lamellar thickness of the K_{T2} phase at temperatures above 130 °C can also be estimated. On the basis of the heavy metal shadowing method, the single lamellar crystal thickness is about 25 nm. This verifies previous results obtained from WAXD data analyzed by the Sherrer equation. Another piece of evidence is that from our DSC measurements the melting temperature of K_{T2} crystals increases with isothermal temperature between 115 and 140 °C. It then approaches a constant melting temperature of 172 °C (see Figure 9) and remains there above an isothermal crystallization temperature of 140 °C. We may thus conclude that, above this temperature, only the single lamellar crystal forms and the thickness reaches its molecular length limit and forms the extended chain crystals. Therefore, it is evident that the rate minimum at 130 °C in the K_{T2} phase is attributed to a crystal morphological change from the folded-chain spherulitic crystals to the extended-chain single lamellar crystals.

Kinetic Considerations for the Experimental Observations. At least three different issues must be addressed in the explanation of the kinetic behavior in these phase transformations. The first deals with the different transformation kinetics among K_O, K_{T1}, and K_{T2} phase structures. The second involves the different linear growth kinetics within the same K_{T2} crystal structure. The third is associated with a relationship between overall and linear phase transformation kinetics in the K_{T2} phase. First, polymorphs exist in PEFBP-(n=11). Each phase structure (the K_O, K_{T2}, or K_{T1} phase) has its own thermodynamic properties (transition temperature, heat of transition, etc.) and, therefore, its own phase transformation kinetics. In each temperature region, a specific phase grows fastest kinetically. As a result, the kinetic data shown in Figures 2, 3, and 6 indicate that the K_O, K_{T1}, and K_{T2} phases show independent growth rate regions; namely, they are formed individually by their own nuclei. In a specific temperature region; the formation kinetics of a specific phase is governed by the lowest free energy barrier regardless of the thermodynamic stability of the phase formed after the barrier is overcome. In other words, the molecules are "blind" and cannot predict the thermodynamic outcome behind the free energy barrier. When they face several free energy barriers, most of the molecules will choose to overcome the lowest free energy barrier, since thermal fluctuations are the only driving force for the molecules to overcome the barrier. As soon as the barrier is overcome and a phase is formed, the molecules are trapped into a state which may be a metastable state, and other activated processes may be

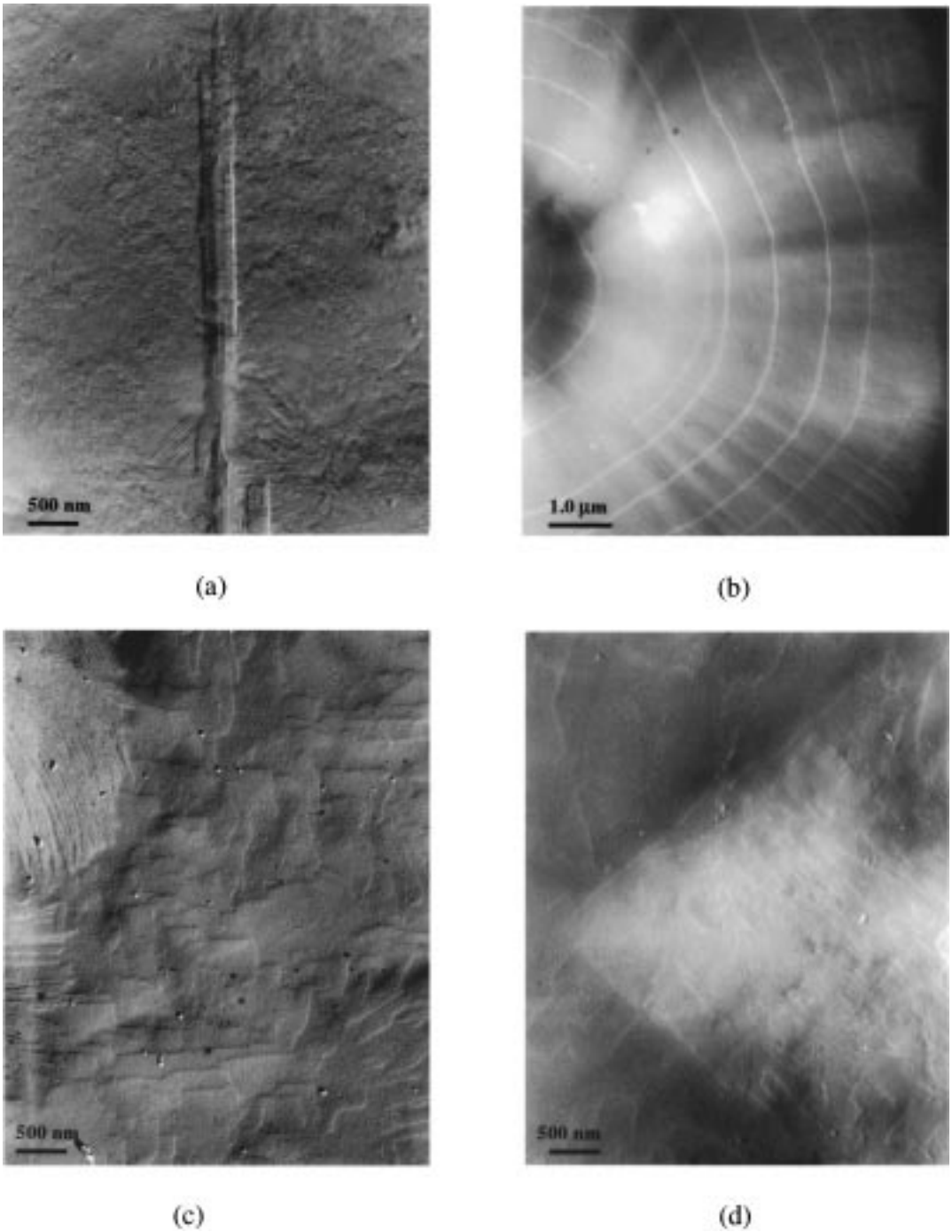

Figure 8. Morphological observations under TEM at different temperatures: (a) the K_O phase at 70 °C; (b) the K_{T1} phase at 100 °C; (c) the K_{T2} phase at 130 °C; (d) single crystals of the K_{T2} phase at 145 °C.

required to reach the ultimate, thermodynamically stable equilibrium state.[16,17]

The second issue is to understand why the two linear growth rate branches appear within the same K_{T2} structure, as shown in Figures 6. For other crystalline polymers, it has been found that different morphologies and even different molecular conformations may also cause the transformation rate minimum, such as in the cases of *n*-alkanes[18,19] and low-molecular-weight α,ω-methoxypoly(ethylene oxide),[20] where a transition from the folded-chain crystals to the extended-chain crystals occurs. Other cases include one of the members of the poly(ether ketone ketone) family, where the lamellar thickness of the crystals may play an important role in the rate minimum behavior.[21] In this study, we have provided an example that the rate minimum can be observed as a chain conformation change during the phase transformation from the folded-chain to the extended-chain crystals. It is particularly interesting from this observation that the rate-minimum is very clearly found in the linear growth rate measurements and is much less clear in the case of the overall transformation rate measurements.

To illustrate this rate minimum, one may also invoke the concept of two free energy barriers for the K_{T2} crystal growth: one is for folded-chain crystals, and the other is for extended-chain crystals. Below 130 °C, the growth barrier of the folded-chain crystals is lower than that of the extended-chain crystals, and thus, most of the molecules overcome this barrier to form the folded-

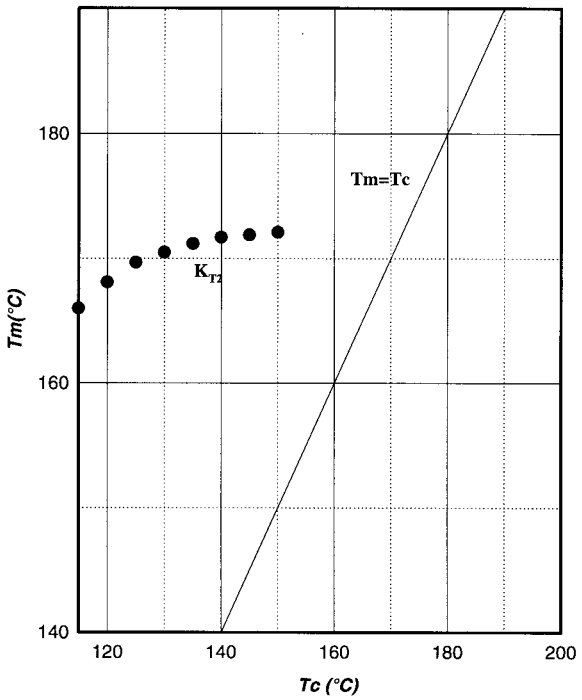

Figure 9. Relationship between the melting temperature and the isothermal crystallization temperature for the K_{T2} phase measured by DSC experiments.

chain crystals even though they are in a metastable state with respect to the extended-chain crystals. Above this temperature, the growth barrier heights are reversed, and therefore, most of the molecules overcome the growth barrier of the extended-chain crystals. In the vicinity of 130 °C, both growth barriers are roughly identical but neither of them is low enough for molecules to easily overcome. As a result, the transformation rates decrease. Therefore, a necessary condition of the appearance of a rate minimum is more than one free energy barrier from which molecules are able to choose. The heights of these barriers rely critically on the undercooling dependence of each barrier. Only when a proper combination between two barriers exists can the rate minimum be seen. Note that these free energy barriers consist of both enthalpy and entropy terms and that, therefore, contributions of the molecular conformation selections (e.g., folded versus extended) during the phase transformation are also included. Regarding the concept of the "self-poisoning" effect,[22] one expects that the "wrong" deposition of the folded chain conformations on the extended-chain crystal surface may substantially hamper further growth by increasing the free energy barrier for the successive molecules to crystallize. A detailed discussion of the molecular kinetic pathways is required to understand how a molecule may overcome the growth barrier which is affected by the crystal surfaces consisting of different molecular topologies.

The third issue in this study deals with the fact that the primary nucleation barrier seems to be different from the growth barriers. As shown in Figures 2 and 3, there is no significant increase of the overall transformation rate above 125 °C. This indicates that although linear growth rates of the extended-chain crystals in the K_{T2} phase can be substantially enhanced (Figure 6), the overall transformation rates which include both the nucleation and growth steps are not; namely, the primary nucleation barrier for the extended-chain crystals must be much higher than the growth barrier, and this is offset by the fast growth rate. Therefore, one has to investigate both the overall transformation and the linear growth rates in order to obtain complete experimental results for providing an understanding of the phase transformation kinetics in this type of complicated system. Although quantitative descriptions of the kinetics are still unavailable, we can see the conceptually important issues.

Conclusion

We have reported complicated phase transformation kinetics in PEFBP(n=11). Isothermal DSC experiments provide the overall transformation kinetics in these three K_O, K_{T1}, and K_{T2} phases. It is evident that there are three distinguishable regions of the overall transformation rates, which correspond to three different phase structures confirmed using WAXD experiments. Two temperatures which represent boundaries between the different regions are found at 95 and 113 °C. They correspond to the transition temperatures of the $K_O \leftrightarrow K_{T1}$ and the $K_{T1} \leftrightarrow K_{T2}$ phases. Linear growth rates for K_{T1} and K_{T2} are measured under PLM while the K_O phase occurs too fast to be detected. An additional result from the linear growth rates is that, within the K_{T2} formation temperature region, a rate-minimum can be observed when the crystal growth morphology changes from folded-chain spherulites to extended-chain single crystals, which have been observed by PLM, TEM, and WAXD experiments. In the temperature region where the extended-chain crystals grow, their melting temperature becomes constant. Discussions of the phase transformation kinetics as well as the rate minimum phenomenon have been offered.

Acknowledgment. This work was supported by the National Science Foundation (Grant DMR-96-17030) and the Science and Technology Center for Advanced Liquid Crystal Optical Materials (ALCOM) at Kent State University, Case Western Reserve University, and the University of Akron. Special thanks should be extended to Mettler-Toledo Company for its support in setting up a DSC-820 in our laboratory.

References and Notes

(1) Herrmann-Schonherr, O.; Wendorff, J. H.; Ringsdorf, H.; Tschirner, P. *Macromol. Chem. Rapid Commun.* **1986**, *7*, 791.
(2) Ballauff, M.; Schmidt, G. F. *Macromol. Chem. Rapid Commun.* **1987**, *8*, 93.
(3) Adam, A.; Spiess, W. *Macromol. Chem. Rapid Commun.* **1990**, *11*, 249.
(4) Kricheldorf, H. R.; Domschke, A. *Macromolecules* **1996**, *29*, 1337.
(5) Watanabe, J.; Sekine, N.; Nematsu, T.; Sone, M.; Kricheldorf, H. R. *Macromolecules* **1996**, *29*, 4816.
(6) Reck, B.; Ringsdorf, H. *Macromol. Chem. Rapid Commun.* **1985**, *6*, 291.
(7) Reck, B.; Ringsdorf, H. *Macromol. Chem. Rapid Commun.* **1986**, *7*, 389.
(8) Zental, R.; Recket, G.; Reck, B. *Liquid Cryst.* **1987**, *2*, 83.
(9) Endres, B. W.; Ebert, M.; Webdorff, J. H.; Reck, B.; Ringsdorf, H. *Liquid Cryst.* **1990**, *7*, 217.
(10) Kappitza, Z.; Zental, R. *Macromol. Chem.* **1991**, *192*, 1859.
(11) Ge, J. J.; Zhang, A.; McCreight, K. W.; Ho, R.-M.; Wang, S.-Y.; Jin, X.; Harris, F. W.; Cheng, S. Z. D. *Macromolecules* **1997**, *30*, 6498.
(12) Wang, S.-Y. Ph.D. dissertation, Department of Polymer Science, The University of Akron, Akron, OH 44325-3909, 1995.
(13) Demus, D.; Richter, L. *Texture of Liquid Crystals*, Weinheim: New York, 1978.

(14) Lovinger, A. J.; Lotz, B.; Davis, D.; Padden, F. J., Jr. *Macromolecules* **1993**, *26*, 3494.
(15) Rodriguez-Arnold, J.; Bu, Z.; Cheng, S. Z. D.; Hsieh, E. T.; Johson, T. W.; Geerts, R. G.; Palackal, S. J.; Hawley, G. R.; Welch, M. B. *Polymer* **1994**, *35*, 5194.
(16) Keller, A.; Cheng, S. Z. D. *Polymer*, in press.
(17) Cheng, S. Z. D.; Keller, A. *Ann. Rev. Mater. Sci.* **1998**, *28*, 533.
(18) Ungar, G.; Keller, A. *Polymer* **1987**, *27*, 1835.
(19) Sutton, S. J.; Vaughan, A. S.; Bassett, D. C. *Polymer* **1996**, *37*, 5735.
(20) Cheng, S. Z. D.; Chen, J. *J. Polym. Sci., Polym. Phys. Ed.* **1991**, *29*, 311.
(21) Blundell, D. J.; Liggat, J. J.; Flory, A. *Polymer* **1992**, *28*, 2475.
(22) Sadler, D. M. *Polymer* **1987**, *28*, 1440.

MA980285O